Photodissociation of $ClONO_2$: 1. Atomic Resonance Fluorescence Measurements of Product Quantum Yields

Leah Goldfarb,[†] Anne-Marie Schmoltner,[‡] Mary K. Gilles, James B. Burkholder, and A. R. Ravishankara*,[†]

National Oceanic and Atmospheric Administration, Aeronomy Laboratory, 325 Broadway, Boulder, Colorado 80303, and Cooperative Institute for Research in Environmental Sciences, University of Colorado, Boulder, Colorado 80309

Received: March 4, 1997; In Final Form: May 22, 1997[⊗]

The quantum yields for the production of Cl, O, and ClO in the photolysis of $ClONO_2$, measured by detecting Cl and O atoms by atomic resonance fluorescence, are reported. The resonance fluorescence signals were calibrated by generating known concentrations of Cl and O atoms from the photolysis of Cl_2, HCl, O_3, or N_2O. The quantum yields for Cl in the 193.2, 222.0, 248.25, and 308.15 nm photolysis of $ClONO_2$ were 0.53 ± 0.10, 0.46 ± 0.10, 0.41 ± 0.13, and 0.64 ± 0.20, respectively. The yields for O atoms at these wavelengths were, respectively, 0.37 ± 0.08, 0.17 ± 0.05, <0.10, and <0.05. The quoted uncertainties are 2σ precision of the measurements. ClO radical was converted to Cl *via* addition of NO and its signal compared to the Cl atom signal produced by photolysis of $ClONO_2$. The obtained quantum yields for ClO were 0.29 ± 0.20, 0.64 ± 0.20, 0.39 ± 0.19, and 0.37 ± 0.19, at 193.2, 222.0, 248.25, and 308.15 nm, respectively. It appears that Cl + NO_3 and ClO + NO_2 are the major products in the photodissociation of $ClONO_2$, except at 193 nm. The measured quantum yields were found to be independent of pressure (40−100 Torr) and bath gas (He and N_2). Our results are compared with those from previous measurements.

Introduction

Rowland *et al.*[1,2] were the first to propose that chlorine nitrate, $ClONO_2$, could be an important temporary reservoir for reactive chlorine in the stratosphere and its formation could reduce the efficiency with which chlorine destroys ozone in this region. Since then, numerous laboratory studies have been carried out to elucidate the chemistry of $ClONO_2$ in the stratosphere.[3,4] Following the first detection of $ClONO_2$ in the stratosphere by Murcray and coworkers,[5] various field measurements have ascertained the abundance of $ClONO_2$ as a function of location and season.[6−11] On the basis of field data, laboratory measurements, and modeling calculations, it is now recognized that the NO_x and ClO_x cycles are strongly coupled through the formation of $ClONO_2$ and this coupling has greatly changed the calculated stratospheric O_3 losses due to NO_x and chlorine perturbations.

$ClONO_2$, formed in the stratosphere by the association reaction

$$ClO + NO_2 + M \rightarrow ClONO_2 + M \quad (1)$$

has many possible loss processes in the stratosphere. The major loss processes[12] for $ClONO_2$ include photolysis,

$$ClONO_2 \xrightarrow{h\nu} \text{products} \quad (2)$$

and heterogeneous reactions,

$$ClONO_2 + H_2O \xrightarrow{\text{PSCs/Sulfuric acid aerosols}} HOCl + HNO_3 \quad (3)$$

$$ClONO_2 + HCl \xrightarrow{\text{PSCs/Sulfuric acid aerosols}} Cl_2 + HNO_3 \quad (4)$$

Reactions with OH, O, and Cl may also contribute to a small extent:

$$OH + ClONO_2 \rightarrow \text{Products} \quad (5)$$

$$Cl + ClONO_2 \rightarrow Cl_2 + NO_3 \quad (6)$$

$$O + ClONO_2 \rightarrow ClO + NO_3 \quad (7)$$

The exact contributions of the photochemical processes to the overall loss of $ClONO_2$ vary with latitude, time of day, season, temperature, and stratospheric sulfuric acid aerosol loading. Currently, it is estimated that photolysis is the major loss channel, except under polar winter conditions.[12,13]

The energetically allowed photodissociation channels for $ClONO_2$ above 200 nm are

$$ClONO_2 \xrightarrow{h\nu} ClO + NO_2 \qquad \lambda < 1066 \text{ nm} \quad (2a)$$

$$\xrightarrow{h\nu} Cl(^2P) + NO_3 \qquad \lambda < 697 \text{ nm} \quad (2b)$$

$$\xrightarrow{h\nu} Cl(^2P) + NO + O_2 \qquad \lambda < 636 \text{ nm} \quad (2c)$$

$$\xrightarrow{h\nu} ClONO + O(^3P) \qquad \lambda < 426 \text{ nm} \quad (2d)$$

$$\xrightarrow{h\nu} Cl(^2P) + NO_2 + O(^3P) \qquad \lambda < 314 \text{ nm} \quad (2e)$$

$$\xrightarrow{h\nu} ClO + NO + O(^3P) \qquad \lambda < 286 \text{ nm} \quad (2f)$$

$$\xrightarrow{h\nu} ClONO + O(^1D) \qquad \lambda < 254 \text{ nm} \quad (2g)$$

$$\xrightarrow{h\nu} Cl(^2P) + NO_2 + O(^1D) \qquad \lambda < 210 \text{ nm} \quad (2h)$$

In the lower stratosphere, where $ClONO_2$ is most abundant, the major photolysis pathways will be one or more of channels 2a−e because the overhead ozone filters out radiation at wavelengths less than 290 nm. However, processes 2f−h may be important in laboratory studies.

[†] Also affiliated with the Department of Chemistry and Biochemistry, University of Colorado, Boulder, CO 80309.

[‡] Present address: National Science Foundation, Division of Atmospheric Sciences, Arlington, VA 22230.

* Author to whom correspondence should be addressed: NOAA R/E/AL2, 325 Broadway, Boulder, CO 80303.

[⊗] Abstract published in *Advance ACS Abstracts,* July 15, 1997.

S1089-5639(97)00818-9 CCC: $14.00

TABLE 1: Quantum Yields for Different Products in the Photodissociation of $ClONO_2$ Reported Prior to 1990

measured species	method	wavelength (nm)	Φ(O)	Φ(Cl)	Φ(ClO)	Φ(NO_3)	ref
end products	indirect	302	major				29
Cl	mass spectrometry	broad band 320 ± 60		major			30
O(^{3}P), Cl(^{2}P)	resonance fluorescence	broad band	large	<0.04			31
end products	indirect	265, 313				0.9	32
NO_3	visible absorption	249				0.55	33
O(^{3}P), Cl(^{2}P)	resonance fluorescence	266, 355	0.1	0.9	small		17
NO_3	visible absorption	254				1[a]	21

[a] Reported that the quantum yield for dissociation decreased with increasing pressure of $ClONO_2$.

The UV absorption spectrum of $ClONO_2$ and its temperature dependence has been studied in the laboratory.[1,13,14] The UV absorption spectrum shows broad structureless features and suggests overlapping multiple electronic transitions; therefore, different dissociation products are possible at different wavelengths. Knowledge of the photodissociation products at wavelengths accessible in the stratosphere is essential for quantifying the role of $ClONO_2$ in determining the abundance of ozone in this region of the atmosphere. For example, the efficiency of chlorine in destroying stratospheric ozone depends on the following catalytic cycle:

$$ClO + NO_2 \xrightarrow{M} ClONO_2 \quad (1)$$

$$ClONO_2 \xrightarrow{h\nu} Cl + NO_3 \quad (2b)$$

$$NO_3 \xrightarrow{h\nu} NO + O_2 \quad (8)$$

$$Cl + O_3 \rightarrow ClO + O_2 \quad (9)$$

$$NO + O_3 \rightarrow NO_2 + O_2 \quad (10)$$

$$\text{Net: } 2\,O_3 \rightarrow 3\,O_2 \quad (11)$$

$ClONO_2$ will not be a part of a catalytic ozone destruction cycle if it is photolyzed *via* channels 2a,d,e. If the photolysis proceeds *via* channel 2c, the efficiency of the ozone destruction cycle will be larger than if it occurred *via* channel 2b. This is because channel 2c will bypass production of NO_3 and directly lead to NO. The quantum yield for NO production in the photolysis of NO_3 varies with altitude and solar zenith angle, but is, for the most part, less than 15% in the lower atmosphere.[15]

The measurements of quantum yields, Φ, of various photoproducts from $ClONO_2$ photolysis have been the subject of a number of laboratory investigations. The main conclusions from the studies carried out prior to 1990 are listed in Table 1. The general conclusion from the pre-1990 studies was that the Cl−O bond, as opposed to the weaker ClO−NO_2 bond, in $ClONO_2$ was broken during photolysis. In 1992, DeMore *et al.*[16] recommended a quantum yield of 0.9 for the Cl + NO_3 channel, and a complementary value of 0.1 for the O + ClONO/$ClNO_2$ channel. This recommendation was derived primarily from Margitan's work[17] at 266 and 355 nm and was deemed appropriate for the wavelength range of 266−355 nm; this is the appropriate wavelength range for the lower and midstratosphere.

This recommendation was reassessed after the more recent studies. Minton *et al.*[18] photolyzed $ClONO_2$ in a molecular beam, a collision-free environment, and reported the ratio of the quantum yields for channels 2a and 2b. Assuming that the quantum yield for the dissociation of $ClONO_2$ was unity and that for other products were negligible, the quantum yields at 248 nm of 0.46 ± 0.08 for the ClO + NO_2 channel and 0.54 ± 0.08 for the Cl + NO_3 channel were calculated. For photolysis at 193 nm, their measured ratio lead to 0.36 ± 0.08 and 0.64 ± 0.08 for the quantum yields for channels 2a and 2b, respectively. In a follow-up study,[19] they reported yields of 0.67 ± 0.06 (Cl + NO_3) and 0.33 ± 0.06 (ClO + NO_2) for 308 nm photolysis. Nickolaisen *et al.*[20] used broad-band photolysis and observed the formation of NO_3 and ClO at $\lambda > 200$ nm as well as at $\lambda > 300$ nm. Unlike the majority of previous studies, Nickolaisen *et al.* reported that the photodissociation quantum yield of $ClONO_2$ decreased with increasing bath gas pressures. They attributed this decrease to the formation of a metastable state of $ClONO_2$ upon photolysis and the collisional quenching of this species by the bath gas prior to its decomposition. Burrows *et al.*,[21] as noted in Table 1, had previously presented some evidence for the dependence of the quantum yields on the pressure of $ClONO_2$. The photolytic lifetime of $ClONO_2$ will increase with increasing pressure if the quantum yield for its loss is pressure dependent and will have significant consequences in the stratosphere. Tyndall *et al.*[22] have also determined quantum yields of Cl and O atoms, detected *via* resonance fluorescence, to be ∼0.75 and <0.05, respectively, at 308 nm. They added NO to convert ClO to Cl and obtained a yield of 0.28 for ClO.

The work described here and in the companion paper was initiated as a comprehensive study of the quantum yields in the photodissociation of $ClONO_2$ as a function of wavelength. In this paper, we report the quantum yields for the production of Cl, O, and ClO at 193.2, 222.0, 248.25, and 308.15 nm. The companion paper reports the quantum yields for NO_3 at 193.2, 248.25, 308.15, and 352.5 nm, compares our results with those from previous studies, and discusses the atmospheric implications of our findings.

Experimental Section

Possible products in the photolysis of $ClONO_2$, reaction 2, include the atomic species Cl(^{2}P), O(^{3}P), and O(^{1}D) and the molecular species ClO, NO_2, NO_3, NO, O_2, and ClONO. (The thermodynamic thresholds at 298 K were calculated using the enthalpies given in DeMore *et al.*).[3] Direct measurements of the quantum yields of the atomic species and indirect measurements of the quantum yields for the ClO radical are described here.

The determination of the quantum yield of a photoproduct requires measuring its concentration upon photolysis and knowing the concentration of the photolyte that absorbed light. The concentrations of the photoproducts were directly measured during these experiments. The concentration of the $ClONO_2$ that absorbed light was calculated using its known absorption cross section at the photolysis wavelength and the photon fluence. All needed absorption cross sections are available in the literature and are listed in Table 2. The photolysis laser fluence in the reactor was determined by actinometry and is described below.

The resonance fluorescence (RF) apparatus which was used in this study to detect Cl and O atoms has been extensively used in our laboratory and is described in detail elsewhere.[23−25] Here, we present only the modifications made to the apparatus to carry out this study and certain key aspects needed to describe fully the conditions for the quantum yield measurements.

TABLE 2: Absorption Cross Sections Used in This Work in Units of 10^{-18} cm^2 molecule^{-1}

	λ (nm)							
compound	184.9	193.2	213.9	222.0	248.25	253.7	308.15	ref
$ClONO_2$		4.64	3.39	3.14	0.616		0.0181	13
O_3		0.434		2.2	10.8	11.6	0.134	34
N_2O		0.0895						3
HCl	0.324	0.0869						3
NO_2							0.17	35
OClO							1.2	36
Cl_2							0.17	3

Briefly, the RF apparatus consisted of a reaction vessel (volume $\sim$ 150 cm^3) through which a mixture of photolytes in a bath gas were flowed. All the gases were introduced through glass lines and the use of Teflon or stainless steel was minimized to suppress the heterogeneous loss of $ClONO_2$. The atomic species were generated by a UV laser passing orthogonal to the direction of the gas flow to minimize the fraction of the cell contents that was photolyzed and to replenish the photolysis volume with a fresh mixture between photolysis laser pulses. Vacuum UV resonance radiation for either Cl or O atom entered the reaction cell orthogonal to the gas flow and photolysis laser beam directions. The atomic fluorescence was collected perpendicular to the direction of the photolysis and excitation beams and detected by a solar-blind photomultiplier tube (PMT).

Chlorine nitrate is hydrolyzed by water on glass and metal. Some of the previous investigations of reactions involving $ClONO_2$ have been suspected to have suffered from such losses. Therefore, the apparatus, consisting of the reactor, all absorption cells, and plumbing in between, was conditioned by filling it with a few milliTorr of $ClONO_2$ for $\sim$20 min and then flushing it with the dried bath gas before each quantum yield measurement. This conditioning removed most of the water adsorbed on the walls which could heterogeneously convert $ClONO_2$ to HNO_3 and HOCl. This procedure was necessary to prevent the loss of $ClONO_2$ and the production of photolyzable species such as HOCl and HNO_3 in the gas flow.

Three 25 mm diameter absorption cells (100, 10.6, and 100 cm long) were set up in series with respect to the gas flow. The first cell was used to measure concentrations of $ClONO_2$ using the 213.9 nm line from a Zn lamp. The following two cells were used to measure O_3 and HCl using the 253.7 and 184.9 nm lines from a Hg lamp. The atomic lines from the lamps were isolated using suitable band-pass filters and detected by photodiodes. The concentrations of all other compounds, in particular NO, Cl_2, and N_2O, were calculated from mass flow rates, measured using calibrated flow meters, and from the pressure in the system. The pressure of the gases flowing through the system was measured at the reactor as well as at the midpoint of the absorption cells using capacitance manometers.

A diluent gas, usually He, was introduced upstream of all other gases. Chlorine nitrate was introduced into the flow at the entrance to the first absorption cell by passing ultrahigh purity (UHP) He through a chlorine nitrate sample which was maintained at 195 K. Helium was dried by passing it through a liquid nitrogen trap prior to entering the chlorine nitrate container. When necessary, ozone was introduced upstream of the second absorption cell and HCl was introduced upstream of the third cell. The photolytes, O_3, $ClONO_2$, HCl, or N_2O, were flowed one at a time so that there was no interference from another absorber in measuring their concentrations *via* UV absorption. For determining the quantum yields of ClO, NO was introduced at the entrance to the photolysis cell.

The linear flow velocity of the gas mixture through the apparatus was typically 20 cm s^{-1}, and was varied from 12 to 40 cm s^{-1}. Results were generally found to be independent of linear flow velocity. For the typical flow velocity employed here, the total residence time of $ClONO_2$ in the entire system was about 20 s. Under these conditions at 298 K, less than 0.1% of the $ClONO_2$ underwent thermal gas phase decomposition in the apparatus.

Operation of the Cl and O atom resonance lamps has been described previously.[23−25] The space between the reactor and the PMT was flushed with dry nitrogen. While Cl atoms were detected, N_2O was added to the N_2 flush; N_2O absorbed O atom radiation without significantly affecting the Cl atom radiation. A CaF_2 window was placed in front of the PMT to prevent detection of Lyman-α radiation, which is unavoidably produced in the microwave discharge lamps. By this method, we could selectively detect Cl atoms in the presence of O and H atoms. Similarly, O atoms could be selectively detected in the presence of H atoms. The O atom lamp was not contaminated with Cl atom radiation.

The output of the PMT was fed to an amplifier−discriminator, and the output of the discriminator was counted by a multichannel scaler. Dwell times of 2−100 μs were used. Data acquisition was initiated before the laser pulse to characterize the background levels of scattered light. Changes in the background counts reflected variations in the detection efficiency, either due to attenuation by or fluorescence of the photolyte or variations in the resonance lamp output. During the course of these experiments, the detection limit was 2×10^8 atom cm^{-3} for oxygen and 5×10^8 atom cm^{-3} for chlorine for an integration time of 1 s. Between 50 and 6000 temporal profiles were coadded to improve the signal to noise ratios.

All photolysis experiments were carried out at room temperature ($T = 297 \pm 1$ K), except for one measurement at 212 K of the chlorine atom yield at 308 nm. No effect of temperature on the quantum yield was observed. In nearly all experiments, the photolysis laser repetition rate was 10 Hz, but a few studies were carried out at 5 Hz to check if incomplete removal of the gas mixture from the photolysis volume affected the measured yields. No difference in quantum yields was observed at the lower laser repetition rate.

Helium was used as the carrier gas in most experiments, with a typical total pressure of 50 Torr. In some instances, the pressure was varied between 40 and 100 Torr. To determine if detectable amounts of O(^{1}D) were produced in the 248 nm photolysis of $ClONO_2$, N_2 was added to the gas stream to quench O(^{1}D) atoms to O(^{3}P).

Excimer lasers (ArF, KrCl, KrF, and XeCl) were used in this study as photolysis light sources. These laser beams are not monochromatic and their outputs cover significant wavelength ranges, up to 2 nm in the case of XeCl laser. The exact effective wavelengths for photolysis are determined by the absorption cross sections of the photolytes and the variation of the fluence with wavelength, as discussed in the companion paper.[26] We used the values of 248.25 nm for KrF, 308.15 nm for XeCl, 222.0 nm for KrCl, and 193.2 nm for ArF. The ranges of laser fluence used in this study were 0.4−4, 1−5, 4−13, and 2−25 mJ cm^{-2} pulse^{-1} at 193, 222, 248, and 308 nm, respectively. One set of $ClONO_2$ photolysis experiments was carried out using the fourth harmonic of a Nd:YAG laser (266 nm) to directly compare our results with those from Margitan.[17]

It was not necessary to externally measure the exact fluence of the lasers since actinometry experiments were carried out. Yet, we monitored the output of the lasers using either a pyroelectric or a photodiode detector. This monitoring enabled us to ensure constancy in the laser fluence and make appropriate corrections when small changes occurred. The precision of the

devices used to measure the fluence was approximately ±5% at the 95% confidence level.

Materials. Chlorine nitrate was synthesized[27] by reacting Cl_2O with an excess of N_2O_5 and warming the sample from 203 to 263 K over a 20 h period. Subsequent distillation of the synthesized chlorine nitrate yielded a sample that contained small amounts of impurities, which were quantified using a 0.5 m spectrometer/diode array detector (with a resolution of 0.5 nm) and/or a chemical ionization mass spectrometer (CIMS). Three separate samples of chlorine nitrate were used during the course of this study. The impurity contributions to the measured quantum yields are discussed later. Ozone was prepared with a commercial ozonizer and stored on silica gel at 197 K. The ozone was then allowed to volatilize into a preconditioned, blackened 12 L bulb. Oxygen was removed from the O_3 *via* repeated freeze−pump−thaw cycles; the purified ozone was diluted in He. A mixture of 500 ppmv (ppmv: parts per million by volume) Cl_2 (electronic grade, >99.97% pure) in UHP He was diluted with dried UHP He for use in the resonance lamp. The diluent gases used in the reactor, UHP He (>99.9995%) and N_2 (>99.9995%), were dried before use. N_2 (>99.98%) and N_2O (99.99%) employed as flush gases were used as supplied by the vendor. NO was separated from its higher oxides by passing it through a silica gel trap at 195 K before use. A mixture of electronic grade HCl (>99.995%) in UHP He was used as supplied.

The variation of the resonance fluorescence signal with concentrations of the atoms were measured by photolyzing a fixed concentration of a photolyte and changing the fluence of the photolysis laser. The resonance fluorescence signals were linear over the range used in the present study, $(0.7-38) \times 10^{11}$ and $(2-45) \times 10^{11}$ atom cm^{-3}, respectively, for Cl and O.

Results

Two methods were used to determine the quantum yields of Cl and O atoms. The postphotolysis atomic resonance fluorescence signal from $ClONO_2$ was compared with that from a reference compound or with that from $ClONO_2$ photolysis at a wavelength where the quantum yield had already been determined. ClO yields were determined by converting it to Cl *via* the addition of an excess of NO. The details of each of these methods and the results are given below in separate sections.

Reference Compound Method. In back-to-back experiments, known concentrations of $ClONO_2$ and a reference compound, O_3, N_2O, Cl_2, or HCl, were photolyzed while keeping the laser fluence, gas flow rates, the resonance lamp output, and the system pressure essentially constant.

The initial concentration of atomic species X produced upon photolysis of $ClONO_2$ is given by

$$[X] = F\sigma_\lambda(ClONO_2)\Phi_X^\lambda(ClONO_2)[ClONO_2] \qquad (I)$$

where F is the laser fluence (defined here as photons $pulse^{-1}$ cm^{-2}), $\sigma_\lambda(ClONO_2)$ is the absorption cross section of $ClONO_2$ at the photolysis laser wavelength λ, and $\Phi_X(ClONO_2)$ is the quantum yield of species X at λ. A similar relationship holds for the reference compound. It follows from these relations that the quantum yield for a species in the $ClONO_2$ photolysis is given by

$$\Phi_X^\lambda(ClONO_2) = \frac{S_{ClONO_2}}{S_{Ref}} \frac{F(Ref)_\lambda}{F(ClONO_2)_\lambda} \frac{[Ref]}{[ClONO_2]} \frac{\sigma_\lambda(Ref)}{\sigma_\lambda(ClONO_2)} \Phi_X^\lambda(Ref) \qquad (II)$$

where S is the signal level (in arbitrary units),Φ is the quantum yield of O or Cl in the photolysis of $ClONO_2$ or the reference compound, and σ_λ is the absorption cross section at the photolysis wavelength λ for $ClONO_2$ or the reference compound. The value of S, the signal after photolysis, was obtained by extrapolating the measured signal as a function of time to t_0, the time at which the photolysis laser fired. In most cases, the extrapolation was for ~20 μs and never more than 100 μs. The error in the signal associated with the extrapolation was less than 2%. Examples of the measured temporal profiles of O and Cl atoms and their extrapolations to time zero are shown in Figure 1. The temporal profiles were generally exponential. The first-order rate coefficients for the loss of Cl and O atoms were measured, and they were in agreement with the known rate coefficients for the reactions of Cl and O atoms with $ClONO_2$ or with the reference compound. In the case of O atoms, the temporal profiles obtained by the photolysis of $ClONO_2$ were not always strictly exponential. This slight nonexponential loss is attributed to loss of O atoms at short times *via* reactions with highly reactive photoproducts. In such cases, only the initial profile was extrapolated to time zero to obtain the signal S. Equation II was used when no modifications to the recorded signal were needed.

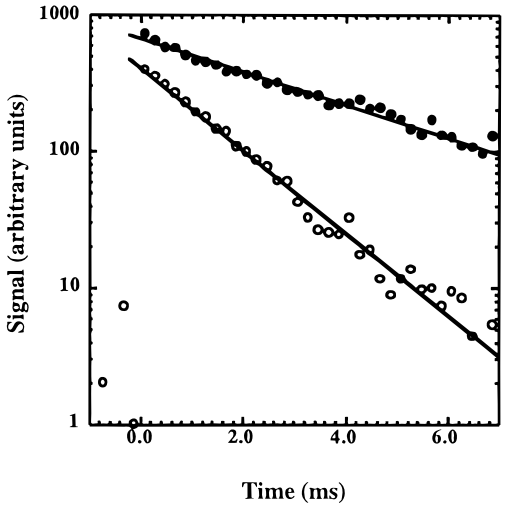

Figure 1. Typical temporal profiles of O atoms (filled circles) and Cl atoms (open circles) obtained in the photolysis of $ClONO_2$. The time scale for the Cl atom loss has been multiplied by 10. Lines are linear least-squares fit of the data to the expression $\ln(S_t) = \ln(S_{t_0}) + k't$. The data was extrapolated to t_0, the time of photolysis, to obtain S_{t_0} (referred to as S in the text), the signal due to photolytically produced O and Cl atoms. (see text).

$ClONO_2$, HCl, Cl_2, and O_3 absorb the resonance lamp radiation and the fluorescence from the atoms. To measure the quantum yields for Cl atoms at 193.2 and for O atoms at 193.2, 222.0, 248.25, and 308.15 nm, the fluorescence signal was corrected to account for the attenuation of the resonance radiation by the photolyte. The equation that governs the signal level for photolysis of $ClONO_2$ is

$$S = PI_0[X]e^{-(\sigma_{lamp}[ClONO_2]L)} \qquad (III)$$

P is a proportionality factor, I_0 is the unattenuated lamp intensity entering the reactor, L is the pathlength between the resonance lamp and PMT through the reaction volume, and σ_{lamp} is the absorption cross section of $ClONO_2$ at the resonance fluorescence wavelength for either O or Cl. Combining eqs I and III leads to the relationship

$$\ln\left(\frac{S}{F[ClONO_2]}\right) = B - \sigma_{lamp}[ClONO_2]L \qquad (IV)$$

where B is

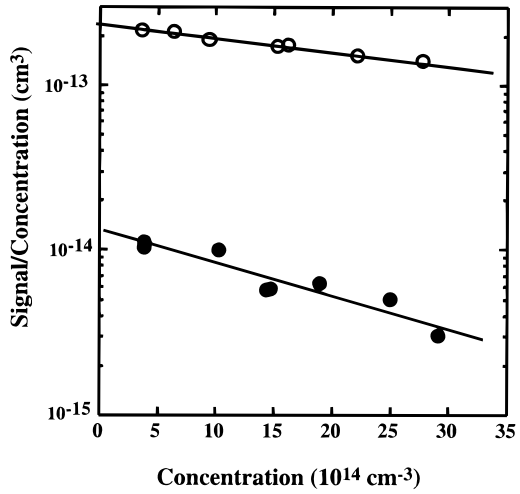

Figure 2. Plots of the initial signals of O atoms from 193.2 nm photolyses of N_2O (open circles) and $ClONO_2$ (filled circles) vs the concentration of the photolytes. The signals were normalized to the concentration of the photolyte. The concentration of N_2O has been multiplied by 10. The lines are the least-squares fit of the data to eq IV. The intercepts yield the *B* parameter.

$$B = \ln(PI_0\sigma_\lambda(ClONO_2)\Phi_X(ClONO_2)) \qquad (V)$$

In the experiments noted above, the initial signals were measured at various concentrations of $ClONO_2$, $\ln(S/(F[ClONO_2]))$ was plotted against $[ClONO_2]$ and the intercept *B* calculated from a linear least-squares fit. Similar experiments were carried out with the reference compounds. Using the two values of the intercepts, the quantum yield was calculated using the relation

$$\Phi_X^\lambda(ClONO_2) = \Phi_X^\lambda(\text{Ref})\,\frac{\sigma_{laser}(\text{Ref})}{\sigma_{laser}(ClONO_2)}\,e^{(B_{ClONO_2}-B_{Ref})} \qquad (VI)$$

Figure 2 shows an example of the variation of the O atom signal with the concentration of $ClONO_2$ and N_2O, the reference photolyte, in the 193 nm photolyses of these compounds. The slopes of these lines are related to the absorption cross section at ~131 nm of the two compounds. The slope in the case of N_2O is consistent with the known cross section at this wavelength.[28] The exact cross sections cannot be calculated because the optical path lengths are not well defined.

For Cl atom quantum yield measurements at 222.0, 248.25, and 308.15 nm, a different approach was used. This approach was necessary because fluorescence signal is absorbed by the photolytes (see Figure 3). The increase in the light scattered by Cl_2 due to resonant scattering prevented the use of background-scattered light as an indicator of the attenuation of the resonance lamp radiation by the photolyte and normalization of the fluorescence signal to small changes in the lamp intensity. The maximum postphotolysis chlorine atom fluorescence signal (adjusted for any change in laser fluence) was plotted *vs* $[ClONO_2]$ or $[Cl_2]$ and fitted to a quadratic expression, as shown in the figure. If there was no attenuation by $ClONO_2$, this plot should be a straight line passing through zero. Instead, the signal increased as $[ClONO_2]$ increased at low concentrations of $ClONO_2$, reached a maximum, and then even decreased slightly when $[ClONO_2]$ was increased further. A similar behavior was seen for Cl_2. The signal that would have been observed in the absence of such attenuation was calculated for a particular concentration ($\sim 4 \times 10^{14}$, an average concentration between that of $ClONO_2$ and Cl_2). The quantum yield for Cl was then calculated using the expression

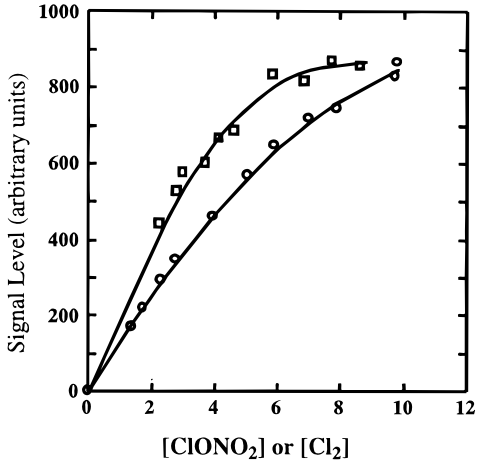

Figure 3. Plots of the initial Cl atom signal from the 308 nm photolyses of $ClONO_2$ (open squares) and Cl_2 (open circles) vs the concentrations of $ClONO_2$ (in units of 10^{14} molecule cm^{-3}) and Cl_2 (in units of 10^{13} molecule cm^{-3}) at a constant laser fluence. The lines are fit of the data to the expression, $y = ax^2 + bx$, where y = signal and x = concentration (See text).

$$\Phi_{Cl}^{308}(ClONO_2) = \frac{S_{ClONO_2}^{corr}}{S_{Cl_2}^{corr}}\,\frac{\sigma_{Cl_2}^{308}}{\sigma_{ClONO_2}^{308}}\,\Phi_{Cl}^{308}(Cl_2) \qquad (VII)$$

where the term S^{corr} for $ClONO_2$ or Cl_2 is the resonance fluorescence signal corrected for the absorption (as above) and any small changes in concentrations of the photolytes and the laser fluence. Note that the concentrations of $ClONO_2$ and the reference compounds were chosen to give similar signal levels whenever it was possible.

The quantum yields measured using the reference compound methods are listed in Table 3 along with the experimental conditions.

Relative Measurement Method. Chlorine nitrate was photolyzed in back-to-back experiments first with a laser at wavelength $\lambda 1$ and then with a laser at wavelength $\lambda 2$ without changing the gas flow velocity, pressure, and the concentration of $ClONO_2$. This method minimized errors characteristic of instrumental instability and drifts in light sources, allowed measurement of quantum yields where suitable reference compounds were not available, and provided an internal check of the other measured values. An aperture was placed before the cell to restrict the radiation of both laser beams to the same area. The laser energy was measured after the photolysis beams exited the reactor. The devices used to measure the laser energy provide accurate ratios (±5%) of the laser energy at the two wavelengths, even though the accuracy at each wavelength may be worse than ±5%. This is because the relative response of the devices with wavelength were calibrated and are traceable to NIST standards.

The postphotolysis signals following irradiation by the two lasers beams were measured in back-to-back experiments. The quantum yield of a species in the photolysis of $ClONO_2$ at wavelength λ_1 is given by the expression

$$\Phi^{\lambda_1} = \Phi^{\lambda_2}\frac{S_{\lambda 1}}{S_{\lambda 2}}\,\frac{F_{\lambda 1}}{F_{\lambda 2}}\,\frac{[ClONO_2]_{\lambda 1}}{[ClONO_2]_{\lambda 2}}\,\frac{\sigma_{\lambda 1}}{\sigma_{\lambda 2}} \qquad (VIII)$$

In the above equation, *S* is the peak signal, *F* is the laser fluence, and σ is the absorption cross section of $ClONO_2$. In most measurements, the concentration of $ClONO_2$ was kept constant, but if it changed measurably, the change was taken into account during data analysis. Under the conditions of constant $ClONO_2$ concentrations, eq VIII can be rearranged to yield

TABLE 3: Summary of Quantum Yields for O and Cl Atoms in the Photodissociation of $ClONO_2$ Measured Using the Reference Compound Method

photolysis wavelength (nm)	ref compd	[ref] (10^{13})[a]	[$ClONO_2$] (10^{14})[a]	no. of expts	quantum yields[b]	pressure/bath gas
			O Atom			
193	N_2O	13−160	5.6−7.4	8	0.35 ± 0.09	40 Torr He + 10 Torr N_2
	N_2O	18−120	4.3−6.3	9	0.39 ± 0.06	40 Torr He + 10 Torr N_2
				av	**0.37 ± 0.05**	
222	O_3	5.2−7.8	2.1−11.1	6	0.16 ± 0.02	40 Torr He + 10 Torr N_2
	O_3	4.3−12	1.5−8.3	6	0.17 ± 0.01	40 Torr He + 10 Torr N_2
				av	**0.17 ± 0.01**	
248	O_3	1.1−8.7	1.3−12	7	0.090 ± 0.004	40 Torr He + 10 Torr N_2
	O_3	0.97−5.2	1.1−8.8	6	0.100 ± 0.005	40 Torr He + 10 Torr N_2
				av	**0.090 ± 0.004**[c]	
308	O_3	0.96−8.8	1.7−17	5	0.0905	50 Torr N_2
					<0.05[d]	
			Cl Atom			
193	HCl	38−520	0.49−5.6	7	0.51± 0.13	50 Torr He
	HCl	95−720	0.77−7.2	9	0.53 ± 0.06	50 Torr He
				av	**0.53 ± 0.06**	
308	Cl_2	1.5−10.2	3−12	7	0.65	50 Torr He
	Cl_2	2.04−11.0	3−12	8	0.78	50 Torr He
	Cl_2	1.71−17.7	2−11	6	0.64	50 Torr N_2
	Cl_2	1.65−9.28	2−14	6	0.65	50 Torr He
	Cl_2	1.5−8.76	4−10	5	0.50	100 Torr N_2
	Cl_2	1.42−22.2	2.6−9	7	0.67	50 Torr He
	Cl_2	1.4−20.7	2−9	9	0.58	50 Torr He[e]
				av	**0.64 ± 0.17**	

[a] Units are molecule cm^{-3}. [b] Reported errors are (2σ) precision. [c] Could have contributions from photolysis of other species (see text). [d] Preferred because of contributions from other sources (see text). [e] At 223 K.

$$\frac{S_{\lambda 1}}{S_{\lambda 2}} = \frac{\Phi^{\lambda_1}}{\Phi^{\lambda_2}} \frac{C_{\lambda 2}}{C_{\lambda 1}} \qquad \text{(IX)}$$

where

$$\frac{C_{\lambda 2}}{C_{\lambda 1}} = \frac{\sigma_{\lambda 2}}{\sigma_{\lambda 1}} \frac{F_{\lambda 2}}{F_{\lambda 1}} \qquad \text{(X)}$$

The relative measurements were carried out for pairs of 248/193, 248/308, and 222/193 nm.

Cl atom quantum yields at 248 and 222 nm were measured relative to those at 193 or 308 nm because a suitable reference molecule which photolyzes at 222 or 248 nm with a known quantum yield for Cl atom production was not available. O atom yields were also determined using this method and served as a check of the yields measured using a reference compound. A plot of $S_{\lambda 1}/S_{\lambda 2}$ vs $C_{\lambda 2}/C_{\lambda 1}$ for Cl atom production (eq IX) from 248 and 308 nm photolyses is given in Figure 4. The slope of this line is the ratio of the quantum yields at 248 and 308 nm. The quantum yields resulting from such measurements are listed in Table 4. The obtained results agree with the values measured using the reference compound method, within the error limits of the two determinations.

Quantum Yields for ClO. ClO produced upon photolysis was converted by NO ([NO] ≫ $[ClO]_0$) to Cl *via* the reaction

$$ClO + NO \rightarrow Cl + NO_2 \qquad (12)$$

($k_{12}(298\ K) = 1.7 \times 10^{-11}$ cm^3 $molecule^{-1}$ s^{-1}).[3] Cl atoms produced directly by $ClONO_2$ photolysis and *via* reaction 12 are lost due to reaction with NO, $ClONO_2$, and other impurities, as well as diffusion out of the viewing zone, and are represented by the reaction 13 as a first order process.

$$Cl \rightarrow \text{loss} \qquad (13)$$

A typical temporal profile obtained in the photolysis of $ClONO_2$ in the presence of NO is shown in Figure 5. Under these conditions, the chlorine atom profiles are governed by the expression:

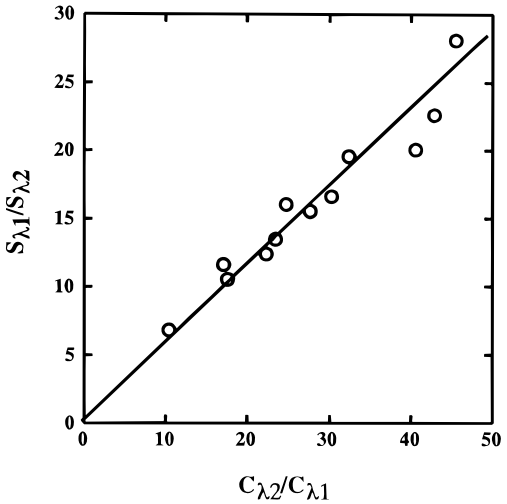

Figure 4. A plot of the ratio of the initial Cl atom signals from the photolyses of $ClONO_2$ at 248.25 and 193.2 nm vs the ratio of parameters $C_{\lambda 2}$ and $C_{\lambda 1}$ (see text). The slope of the line yields the ratio of the quantum yields at the two wavelengths.

$$[Cl]_t = Ce^{-k_{13}t} + De^{-k_{12}^{I}t} \qquad \text{(XI)}$$

where

$$C = [Cl]_0 + \left(\frac{k_{12}^{I}}{k_{12}^{I} - k_{13}}[ClO]_0\right) \qquad \text{(XII)}$$

$$D = \left(\frac{k_{12}^{I}}{k_{13} - k_{12}^{I}}[ClO]_0\right) \qquad \text{(XIII)}$$

and $k_{12}^{I} = k_{12}[NO]$. Temporal profiles of the Cl atom resonance fluorescence signal to eq XI were fit using a nonlinear least-squares-fitting routine to extract $[ClO]_0/[Cl]_0$. Thus, we did not require the knowledge of the absolute concentration but

TABLE 4: Quantum Yields for Cl and O Atoms Measured Relative to those from $ClONO_2$ Photolysis at Another Wavelength

λ (nm)	no. of expts	$[ClONO_2]^a$	ratio	weighted average	Φ
			O Atoms		
222/193	6	1.4−9.9	0.56 ± 0.07	0.58 ± 0.06	0.22 ± 0.08[c,d]
222/193	6	1.9−10.7	0.64 ± 0.11		
248/193[b]	9	0.7−6.0	0.24 ± 0.07	0.29 ± 0.03	0.11± 0.06[d,e,f]
248/193	10	0.9−6.1	0.30 ± 0.04		
			Cl Atoms		
222/193	7	1.8−6.9	0.89 ± 0.08	0.87 ± 0.07	0.46 ± 0.09[c]
222/193	6	1.9−8.9	0.77 ± 0.16		
248/193	12	1.1−7.2	0.79 ± 0.16	0.78 ± 0.10	0.41 ± 0.11[e]
248/193	12	2−6.7	0.78 ± 0.13		
248/308	12	3−8	0.58 ± 0.10	0.58 ± 0.10	0.37 ± 0.20[e]

[a] Units 10^{14} molecule cm^{-3}. [b] No N_2 in the cell. [c] At 222 nm. [d] Value derived from the absolute method is preferred over this relative value. [e] At 248 nm. [f] Could have contributions from photodissociation of other species (see text).

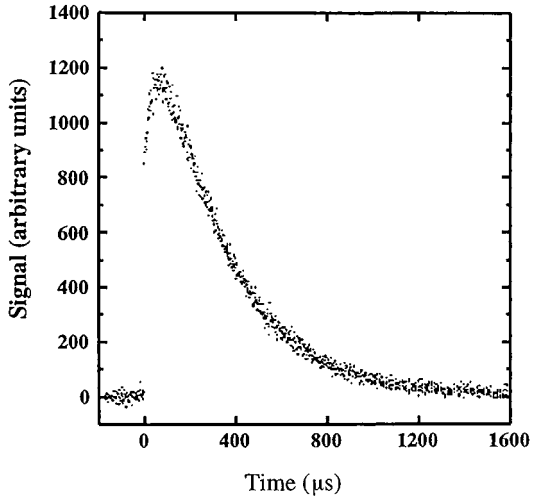

Figure 5. A temporal profile of Cl atoms measured in the 308.15 nm photolysis of a mixture of $ClONO_2$ and NO. The jump at time zero is due to Cl atom from the photolysis of $ClONO_2$ and the subsequent rise is due to reaction 12. Such profiles were analyzed to determine the yields of ClO.

only the relative signal levels. In these experiments, the NO concentrations were varied ($(5-30) \times 10^{14}$ molecule cm^{-3}). In fitting the temporal profiles to eq XI, we also obtained k_{12}^{I} for each fit. From the determined values of k_{12}^{I} and the measured concentrations of NO, k_{12} was calculated to be $(2 \pm 0.5) \times 10^{-11}$ cm^3 $molecule^{-1}$ s^{-1}. This value is close to the recommended value[3,4] of 1.7×10^{-11} cm^3 $molecule^{-1}$ s^{-1} and increases our confidence that the time dependent Cl atom production was due to ClO. The removal of Cl was essentially due to reaction (6) and the Cl + NO + M reaction. The value of k_{13} obtained from the fits was consistent with the calculated first-order rate coefficient for the loss of Cl *via* reactions with $ClONO_2$ and NO using recommended rate coefficients.[3]

Scattered light from the photolysis beam complicated the analysis of the fluorescence signal at 193.2 and 222.0 nm to obtain the yields of ClO. The solar blind PMT has a nonzero response at these shorter photolysis wavelengths and was saturated by the laser pulse for 6−10 μs. Therefore, obtaining the initial signal due to Cl produced from the photolysis required a longer back extrapolation of the measured temporal profiles and was, consequently, less accurate. The ClO production from $ClONO_2$ at 266 nm was also investigated even though the absolute Cl atom yield was not measured. The calculated $[ClO]_0/[Cl]_0$ ratio was 0.8 ± 0.2. The obtained quantum yields for ClO are summarized in Table 5.

Discussion

The measured yields of Cl, O, and ClO are listed in Tables 3, 4, and 5 along with the precision of the measurements. The quoted precision is 2 times the standard deviation of the mean for a set of experiments carried out under similar experimental conditions, but by varying the concentrations of the reference compound and $ClONO_2$. The number of experiments for each set is also shown in the tables. Possible sources of systematic error in measuring these quantum yields were (1) uncertainties in measuring the concentrations of $ClONO_2$ and reference compounds (in the reference compound method), (2) the contribution of impurities that can be photolyzed to yield Cl and O atoms, and (3) errors in the reported quantum yields of the reference compounds. These errors are briefly assessed below.

The concentration of $ClONO_2$ in the gas mixture flowing through the reactor was measured *via* UV absorption at room temperature. We estimate the combined systematic error due to optical path length, pressure measurements, and absorption cross sections to be <5%. The largest contributor to this error is the uncertainty in the absorption cross section at the monitoring wavelengths. Since the value of the cross section is also involved in calculating the number of $ClONO_2$ molecules that absorbed the photolysis laser light, many of the systematic errors associated with the absorption cross sections cancel out in the quantum yield calculations as long as we use the cross sections from the same study. Here we used the values of Burkholder *et al.*[13] for $ClONO_2$ absorption cross sections. The above estimated systematic error due to uncertainties in concentrations should also apply to Cl_2, HCl, and O_3. Concentrations of Cl_2, HCl, and O_3 were also measured *via* UV absorption. As mentioned earlier, decomposition of $ClONO_2$ in the system was minimal (<0.1%) and was neglected. Concentrations measured *via* flow measurements should have systematic errors similar to those measured by absorption.

Synthesized samples of $ClONO_2$ contained trace amounts of impurities. Multiple distillations were carried out to remove a large fraction of the impurities. Yet, small amounts of OClO, NO_2, Cl_2 and Cl_2O remained in our samples. They were quantified, as noted earlier. When the impurity levels were below the detection limit of these systems, their concentrations were assumed to be the detection threshold values. The contributions of the impurities to the measured yields were estimated and they were often upper limits. These estimated contributions are included as uncertainties rather than as corrections to the measured values. This is because the above impurity analyses were for the prepared samples. The impurity levels in the reactor may not be exactly the same due to conversions, in the process of being introduced into the reactor. As the samples were used, they may have even become purer because of fractional distillation. Therefore, the above contribution of impurities may even be an overestimation since the level of the impurities could be smaller than the detection limits assumed. The estimated uncertainties due to impurities are included in the errors listed in Table 6. It should be noted that, because all or a large fraction of the O atoms in the 248.25 and 308.15 nm photolyses could be from the impurities, the O atom quantum yields at these wavelengths are quoted as upper limits.

The reference compounds were chosen because the quantum yields for the production of Cl and O atoms from their photolyses are well-known.[3] The quantum yield for the production of Cl from Cl_2 and HCl and that of O atoms from O_3 and N_2O are assumed to have negligible uncertainties. The overall estimated uncertainties in the measured quantum yields are listed in Table 6.

TABLE 5: Quantum Yields for ClO in the Photodissociation of $ClONO_2$

λ (nm)	ratio range	[NO][a]	[$ClONO_2$][a]	no. of expts	ratio [ClO]/[Cl] (2σ)	average ratios	Φ(ClO)
193	0.52−0.71	3−8	5.5	3	0.61 ± 0.19		
193	0.39	4.6−16	3.3−5.6	8	0.47 ± 0.19	0.54 ± 0.13	**0.29 ± 0.19**
222	0.7−1.4	3−10	4.8	5	1.1 ± 0.56		
222	1.33−1.5	1−4	1−2.1	5	1.4 ± 0.1	1.39 ± 0.1	**0.64 ± 0.19**
248	0.75−1.03	2−25	3.4−7.6	13	0.87 ± 0.18		
248	0.8−1.05	NM[b]	3−6.2	11	0.98 ± 0.13	0.94 ± 0.11	**0.39 ± 0.18**
266	0.69−0.93	4−15	5.5	6	0.81 ± 0.20	0.81 ± 0.20	*c*
308	0.52−0.61	NM[b]	6.6	7	0.57 ± 0.06		
308	0.24−0.76	4.6−36	9−15	4	0.57 ± 0.03	0.57 ± 0.06	**0.37 ± 0.18**

[a] In units of 10^{14} molecule cm^{-3}. [b] NM = Not Measured. [c] Yield of ClO was not calculated because the Cl atom quantum yield at this wavelength was not measured.

TABLE 6: Summary of Quantum Yields for Various Products in the Photolysis of $ClONO_2$ at 298 K

	Quantum Yields					
λ (nm)	Cl	O(^{3}P)	ClO	ClONO	NO_2	comments
260−380	1.0 ± 0.2	0.1	0.04			*a*
200−900	<0.04	>0.04				*b*
266, 355	0.9 ± 0.1	0.1 ± 0.1				*c*
254		0.24		1.0−0.3		*d*
193	0.64 ± 0.08		0.36 ± 0.08		0.36 ± 0.08	*e*
248	0.54 ± 0.08		0.46 ± 0.08		0.46 ± 0.08	*e*
308	0.67 ± 0.06		0.33 ± 0.06		0.33 ± 0.06	*f*
308	0.80 ± 0.20	<0.05	0.28 ± 0.12			*g*
>200			0.61 ± 0.20			*h*
>300			0.44 ± 0.08			
193	0.53 ± 0.10[i]	0.37 ± 0.08[i]	0.29 ± 0.20[i]			
	0.45 ± 0.08[j]	<0.9[k]				
222	0.46 ± 0.10[i]	0.17 ± 0.05[i]	0.64 ± 0.20[i]			
248	0.41 ± 0.13[i]	<0.10[i,j]	0.39 ± 0.19[i]			
	0.60 ± 0.12[j]	<0.4[j]				
266			[l][i]			
308	0.64 ± 0.20[i]	<0.05[j]	0.37 ± 0.19[j]			

[a] Chang *et al.*[30] mass spectrometry. [b] Alder-Golden and Wiesenfeld[31] resonance absorption. [c] Margitan[17] resonance fluorescence. [d] Burrows *et al.*[21] molecular modulated spectroscopy with UV−vis absorption and matrix isolation with FTIR. [e] Minton *et al.*[18] molecular beam/mass spectrometry. [f] Moore *et al.*[19] molecular beam/mass spectrometry. [g] Tyndall *et al.*[22] resonance fluorescence [h] Nickolaisen *et al.*[20] visible absorption spectrometry with broad-band photolysis. [i] Work from our laboratory. Quoted uncertainties include estimated systematic errors. Resonance fluorescence data. [j] Work reported in the companion paper. Quoted uncertainties include estimated systematic errors. UV−visible absorption data.[26] [k] Measured value is taken as an upper limit because other species in the reactor could have contributed to the measured yield. [l] Ratio of ClO/Cl was measured to be 0.8. The yield was not quantified since the quantum yield for Cl at 266 nm was not measured.

The uncertainty in the quantum yields of Cl or O atom measured at one wavelength using the relative method depends on the uncertainty at the second wavelength. Similarly, the uncertainties in the quantum yields of ClO depend on the uncertainties in the Cl atom quantum yields. In the case of ClO yields, there was an additional uncertainty due to the difficulty in determining the signal level at $t = 0$. Scattered light from the laser obscured the Cl atom signals at short times especially at shorter wavelengths. Therefore, the measured longer-time profiles were fit to an exponential rise attributed to the Cl atom production from conversion of ClO to Cl *via* the reaction with NO and extrapolated to $t = 0$. Extensive tests were carried out to characterize the time interval between triggering the data acquisition and the exact time for photolysis. We conservatively estimate this uncertainty to be $<0.5\ \mu$s. The uncertainty associated with the timing was dependent on the first order rate coefficient for the disappearance of ClO; the calculated uncertainty due to the error in time is also included in the errors quoted in the last column of Table 5.

The measured quantum yields were invariant to changes in flow velocity (varied by a factor of three), laser fluence (order of magnitude), and total pressure (50−100 Torr). Thermal decomposition of $ClONO_2$ and the photolysis of the products have been estimated to make an insignificant contribution to the reported quantum yields.

As seen in Tables 3 and 4, the measured ratios of the quantum yields of O and Cl atoms at two different photolysis wavelengths agree with the ratios of the quantum yields measured individually. This agreement suggests that our measured values do not contain any major undetected systematic errors due to concentration determinations and the quantum yields of Cl and O in the photolysis of reference compounds.

In one set of measurements, O atom quantum yields at 248 nm were measured first with N_2 present and then with N_2 absent. The quantum yields, 0.24 ± 0.07 and 0.30 ± 0.04, respectively, were essentially the same. Therefore, we conclude that the yield of O(^{1}D) is insignificant. One of the significant findings from this work was that ClO was indeed a major product in the photodissociation of $ClONO_2$ at and below 308 nm. The largest yield of ClO, 0.6 ± 0.3, was at 222 nm and ranged between 0.3−0.4 at other wavelengths. The rise in Cl atom signal with a time constant expected from the known rate coefficient for the reaction of ClO with NO gives us further confidence that ClO is the source of Cl atoms produced in the presence of NO. Our observation of ClO supports the findings of Minton *et al.*[18] and Moore *et al.*[19] who were the first to report direct detection of ClO in $ClONO_2$ photolysis. These investigators measured the relative yields of the ClO + NO_2 and Cl + NO_3. By assuming that the quantum yield for $ClONO_2$ photodissociation is unity and that the yields of other photoproducts are negligible, the quantum yields for channels 1a and 1b were calculated. As discussed in the companion paper,[26] the measured quantum yields from this study are in agreement with this assertion. Margitan[17] had reported the ClO yield to be small, if not zero. We attempted to repeat his experiment by photolyzing $ClONO_2$ at 266 nm in the presence of NO; copious amounts of ClO were

observed. It should be noted that to observe the formation of Cl from ClO in the presence of $ClONO_2$, the concentration of NO has to be in the range used here. If too little NO is used, the conversion of ClO to Cl will be masked by the loss of Cl *via* reaction with $ClONO_2$. If too much NO is present, the conversion of ClO to Cl occurs too fast and Cl atom rise will be obscured by the direct production from $ClONO_2$ photolysis.

As in the case of many recent studies, we see Cl atoms as a major, though not exclusive, product of the photodissociation of $ClONO_2$ at and below 308 nm. The measurements of the quantum yields for the complementary product, NO_3, are described in the companion paper. Overall, the results from the companion work agree with the findings from this study. This agreement is noteworthy, since the yields were obtained by two different techniques under different conditions.

Unlike our study, where photolysis at individual wavelengths was carried out, Nickolaisen *et al.*[20] used a broad-band light source. They reported photodissociation quantum yields for ClO and Cl. Our results at 308 nm agree, within error bars, with their values for $\lambda > 300$ nm. However, Nickolaisen *et al.* reported that the quantum yield for the dissociation of $ClONO_2$ at longer wavelengths decreased with increases in bath gas pressure. We did not observe any changes in the yields of O and Cl atoms with pressure, albeit over a limited range of 40−100 Torr. Also, the measured quantum yields did not depend on whether the bath gas was He (40 to 100 Torr) or N_2 (50 and 100 Torr). A decrease in the quantum yield with pressure indicates a long-lived excited state and the possibility of exciting such a state at a given wavelength may change with temperature. Therefore, we measured the quantum yield for Cl atoms in the 308 nm photolysis at 223 K. The measured quantum yield, as shown in Table 3, remained unchanged.

In summary, Cl and ClO were found to be the major photodissociation products at wavelengths greater than 222 nm. O atoms, though prominent in the 193 nm photolysis, are a minor product at longer wavelengths. The yield of Cl atoms is nearly the same at all four wavelengths. However, the ClO yield appears to decrease with increasing wavelengths for $\lambda >$ 222 nm. Comparison of these results with those from NO_3 yield determinations are given in the accompanying paper.[26] That paper also includes a discussion of the photolysis pathways and the atmospheric implications of our finding.

Acknowledgment. A.M.S. thanks Y. T. Lee for his continued scientific inspiration. We thank L. Greg Huey for the CIMS analyses. L.G. thanks National Aeronautics and Space Administration for a Global Change Research Doctoral Fellowship. This work was funded in part by the Upper Atmosphere Research Program of the National Aeronautics and Space Administration.

References and Notes

(1) Rowland, F. S.; Spencer, J. E.; Molina, M. J. *J. Phys. Chem.* **1976**, *80*, 2711−2713.

(2) Rowland, F. S.; Spencer, J. E.; Molina, M. J. *J. Phys. Chem.* **1976**, *80*, 2713−2715.

(3) DeMore, W. B.; Sander, S. P.; Golden, D. M.; Hampson, R. F.; Kurylo, M. J.; Howard, C. J.; Ravishankara, A. R.; Kolb, C. E.; Molina, M. J. Chemical Kinetics and Photochemical Data for Use in Stratospheric Modeling, Evaluation No. 12. JPL Publication 97−4; Jet Propulsion Laboratory: Pasadena, CA, 1997.

(4) Atkinson, R.; Baulch, D. L.; Cox, R. A.; Hampson, R. F.; Kerr, J. A.; Troe, J. *J. Phys. Chem. Ref. Data* **1992**, *21*, 1125−1568.

(5) Murcray, D. G.; Goldman, A.; Murcray, F. H.; Murcray, F. J.; Williams, W. J. *Geophys. Res. Lett.* **1979**, *6*, 857−859.

(6) Massie, S. T.; Davidson, J. A.; Cantrell, C. A.; McDaniel, A. H.; Gille, J. C.; Kunde, V. G.; Brasunas, J. C.; Conrath, B. J.; Maguire, W. C.; Goldman, A.; Abbas, M. M. *J. Geophys. Res.* **1987**, *92*, 14806−14814.

(7) Goldman, A.; Murcray, F. J.; Blatherwick, R. D.; Kosters, J. J.; Murcray, F. H.; Murcray, D. G.; Rinsland, C. P. *J. Geophys. Res.* **1989**, *94*, 14945−14955.

(8) Coffey, M. T.; Mankin, W. G.; Goldman, A. *J. Geophys. Res.* **1989**, *94*, 16597−16613.

(9) Toon, G. C.; Farmer, C. B.; Lowes, L. L.; Schaper, P. W.; Blavier, J. F.; Norton, R. H. *J. Geophys. Res.* **1989**, *94*, 16571−16596.

(10) Zander, R.; Gunson, M. R.; Foster, J. C.; Rinsland, C. P.; Namkung, J. *J. Geophys. Res.* **1990**, *95*, 20519−20525.

(11) Roche, A. E.; Kumer, J. B.; Mergenthaler, J. L. *Geophys. Res. Lett.* **1993**, *20*, 1223−1226.

(12) Scientific Assessment of Ozone Depletion: 1994. Global Ozone Research and Monitoring Project. Technical Report No. 37; World Meteorological Organization: Geneva, 1994.

(13) Burkholder, J. B.; Talukdar, R. K.; Ravishankara, A. R. *Geophys. Res. Lett.* **1994**, *21*, 585−588.

(14) Molina, L. T.; Molina, M. J. *J. Photochem.* **1979**, *11*, 139−144.

(15) Johnston, H. S.; Davis, H. F.; Lee, Y. T. *J. Phys. Chem.* **1996**, *100*, 4713−4723.

(16) DeMore, W. B.; Sander, S. P.; Golden, D. M.; Hampson, R. F.; Kurylo, M. J.; Howard, C. J.; Ravishankara, A. R.; Kolb, C. E.; Molina, M. J. Chemical Kinetics and Photochemical Data for Use in Stratospheric Modeling, Evaluation No. 10; JPL Publication 92−2, Jet Propulsion Laboratory: Pasadena, CA, 1992.

(17) Margitan, J. J. *J. Phys. Chem.* **1983**, *87*, 674−679.

(18) Minton, T. K.; Nelson, C. M.; Moore, T. A.; Okumura, M. *Science* **1992**, *258*, 1342−1345.

(19) Moore, T. A.; Okumura, M.; Tagawa, M.; Minton, T. K. *Faraday Discuss. Chem. Soc.* **1995**, *100*, 295−307.

(20) Nickolaisen, S. L.; Sander, S. P.; Friedl, R. R. *J. Phys. Chem.* **1996**, *100*, 10165−10178.

(21) Burrows, J. P.; Tyndall, G. S.; Moortgat, G. K. *J. Phys. Chem.* **1988**, *92*, 4340−4348.

(22) Tyndall, G. S.; Kegley-Owen, C. S.; Orlando, J. J.; Calvert, J. G. *J. Chem. Soc. Faraday Trans.* **1997**, in press.

(23) Turnipseed, A. A.; Vaghjiani, G. L.; Thompson, J. E.; Ravishankara, A. R. *J. Chem. Phys.* **1992**, *96*, 5887−5895.

(24) Thompson, J. E. Kinetics of $O(^1D)$ and $Cl(^2P)$ Reactions with Halogenated Compounds of Atmospheric Interest. M.S. Thesis, University of Colorado, Boulder, 1993.

(25) Warren, R. F.; Ravishankara, A. R. *Int. J. Chem. Kinet.* **1993**, *25*, 833−844.

(26) Yokelson, R. J.; Burkholder, J. B.; Fox, R. W.; Ravishankara, A. R. *J. Phys. Chem.* **1997**, in press.

(27) Schmeisser, M. *Inorg. Syn.* **1967**, *9*, 127.

(28) Hudson, R. D. Critical Review of Ultraviolet Photoabsorption Cross Sections for Molecules of Astrophysical and Aeronomic Interest, National Bureau of Standards, U.S. Department of Commerce, U.S. GPO: Washington, DC, 1991.

(29) Smith, W. S.; Chou, C. C.; Rowland, F. S. *Geophys. Res. Lett.* **1977**, *4*, 517−519.

(30) Chang, J. S.; Barker, J. R.; Davenport, J. E.; Golden, D. M. *Chem. Phys. Lett.* **1979**, *60*, 385−390.

(31) Adler-Golden, S. M.; Wiesenfeld, J. R. *Chem. Phys. Lett.* **1981**, *82*, 281−284.

(32) Knauth, H.-D.; Schindler, R. N. *Z. Naturforsch.* **1983**, *38a*, 893−895.

(33) Marinelli, W. J.; Johnston, H. S. *Chem. Phys. Lett.* **1982**, *93*, 127−132.

(34) Molina, L. T.; Molina, M. J. *J. Geophys. Res.* **1986**, *91*, 14501−14508.

(35) Bass, A. M.; Ledford, A. E.; Laufer, A. H. *J. Res. Nat. Bur. Stand.* **1976**, *80A*, 145−166.

(36) Wahner, A.; Tyndall, G. S.; Ravishankara, A. R. *J. Phys. Chem.* **1987**, *91*, 2734−2738.